

The Effect of Physical and Electrical Properties on the Synthesis of Manganese Oxide Carbon from Leaching Rocks as Supercapacitor Electrodes

ABSTRACT

Manganese rocks are classified into manganese oxide, silicate, and carbonate. The research was carried out to synthesize carbon manganese oxide from the leaching of manganese rock and how to influence the physical and electrical properties of carbon manganese oxide from the leaching of manganese rock as the primary material for supercapacitor electrodes. The highest capacitance value produced was 65.3 μF in the composite ratio MnO_2 : Carbon 0.25 g : 0.75. In the resistance test, the lowest resistance value was obtained in comparing the composite MnO_2 : Carbon 0.25 g : 0.75 g with a resistance value of 1.92 $\text{k}\Omega$. The highest inductance value obtained was 126.7 mH on the composite ratio MnO_2 : Carbon 0.75 g : 0.25 g. In the conductivity test, the highest value was obtained at 60.4 $\mu\text{S cm}^{-1}$ in the composite ratio MnO_2 : carbon 0.75 g : 0.25 g.

Keywords: Manganese; carbon; leaching; FTIR; XRD.

1. INTRODUCTION

Manganese is the fourth most used metal after iron, aluminum, and copper in life daily. Nearly 99% of manganese is used for the steel and iron industry. Manganese dioxide (MnO_2) is a stable compound both under acidic and alkaline conditions, so to process manganese ore, it must be done by a reduction process first using a reducing agent. One of the parameters in the purification of manganese oxide that needs to be considered is the interfering impurities found in manganese ores, such as Fe, Al, Si, and other metals [1]. Manganese deposits are reported in parts of the region, such as the Paludda area, Barru Regency, and South Sulawesi Province.

Manganese ore processing is divided into two parts: pyro-lurgy and hydrometallurgy. Manganese ore with content above 45%, commonly known as a metallurgical grade, is processed pyro-metallurgically to become ferromanganese metal [2-5]. Meanwhile, manganese ore with a content below 45% is used for the production of non-metallurgical grade. Pyrolusite manganese ore can be selectively dissolved in an acidic environment,

and manganese leaching is reductive. In its implementation, certain compounds are needed to reduce the oxidation number of Mn from Mn (VI) to Mn (II) so that it can be dissolved using acidic compounds. About 90% of the manganese oxide can be recovered from the ore with the operating temperature set at 90°C (Slamet et al. 2013).

Hydrometallurgy is a metal processing method from minerals or ores using several solvents, commonly known as leaching. Research to develop hydrometallurgical processes has been carried out using solvents and the addition of several oxidizing agents [6-10]. Several studies have reported that manganese ore can be dissolved in sulfuric acid with recovery rates above 90% [11-15]. Many reducing agents have been developed with efficient processes to recover the recovery percentage of manganese ore, mainly from inorganic (sulfur dioxide) and organic (hydrogen peroxide) materials. Therefore, many studies have focused on refining manganese ore using organic reducing agents because it is environmentally friendly and inexpensive [16].

*Corresponding author: E-mail:

Capacitors include components or devices that can store a large enough electric charge for a while. This capacitor consists of metal plates insulated from each other by insulators [17]. Capacitors are widely used as alternating current filters to direct current, frequency regulators in insulators, electrostatic charge storage, etc. Capacitors are electrical energy storage media that have a large energy density and power density and have a long period, namely supercapacitors [18].

Supercapacitors are energy storage devices that are just as useful as batteries. While batteries use chemical reactions to store energy, supercapacitors generally store energy through the physical separation of electric charges. Supercapacitors are based on carbon (nanotube) technology, and the carbon technology in these capacitors creates a huge surface area with minimal separation. All supercapacitors consist of two electrodes immersed in a conductive solution or conductive polymer called an electrolyte [19-22]. A separator separates the electrodes, commonly called a dielectric material separator, which is not only for the charge on the two electrodes but also has electrical properties that affect the performance of the supercapacitor [23].

Carbon is defined as a material with several advantages in terms of physical and chemical properties, so many researchers are currently developing it. The advantages of this carbon make the carbon material with many applications [24-28]. Morphology dramatically influences the performance of carbons such as graphene, which has synthesis conditions (Rakhmad and Rakhma, 2018). Previous studies have synthesized carbon manganese oxide as the primary material for energy storage media electrodes. Fitriani's research (2017) by synthesizing MnO_2 particles on the surface of corncob-activated carbon (*Zea mays* L.) as a capacitor electrode material in which the results of capacitance measurements show that MnO_2 has a perfect pseudocapacitive effect up to 15,000 times the specific capacitance value of activated carbon before deposition of 0.0066 mF/g. Research by Subagio et al. [29] by synthesizing CNT/ MnO_2 nanocomposites as supercapacitor materials with XRD test results showing an amorphous structural pattern in manganese oxide (MnO_2) material with a diffraction peak appearing at $26.37^\circ C$ which shows the peak of refraction on the bond of CNT material, especially in the composition of 50% CNT/ MnO_2 . Maddu research et al. [30]

synthesized MnO_2 /Carbon Dots nanocomposites from rice husks as supercapacitor electrodes with FTIR test results with functional groups identified in the infrared transmittance spectrum, respectively OH, C=CC \equiv C. The objective of this study is to synthesize carbon manganese oxide from the leaching of manganese rock and how to influence the physical and electrical properties of carbon manganese oxide from the leaching of manganese rock as the primary material for supercapacitor electrodes.

2. RESEARCH METHODS

2.1 Tools and Materials

The tools used in this research are X-Ray Diffraction (XRD), Fourier Transform Infrared (FTIR), LCR-Meter, Acetylene black Conductometer, polyvinylidene fluoride (PVDF), distilled water (H_2O), sulfuric acid (H_2SO_4) 2 M, sodium hydroxide (NaOH) 10%, sodium carbonate ($NaCO_3$).

2.2 Procedure Preparation

The manganese rock used was taken from the Paludda Region, Barru Regency. The manganese rock was washed with distilled water and dried in an oven at $60 - 90^\circ C$ for 2 hours. Then the sample was ground until smooth and sieved using a 150-mesh sieve. It was then stored in a closed container.

1. Leaching of Manganese Ore

Extraction of MnO_2 from manganese ore follows the method of Wahyudi et al. (2013) and Amalia et al. (2016) with slight modifications. A total of 25 g of the prepared sample was added to 500 mL of 2 M H_2SO_4 , stirred at $90^\circ C$, and added 50% molasses as a reducing agent. Leaching time was carried out for 6 hours and stirred using a magnetic stirrer at 300 rpm. Then the mixture was filtered, and the leaching solution was heated at $70^\circ C$. Then, 10% NaOH was added until the pH reached 5 – 6 to precipitate metal impurities. Then the solution was filtered and heated to a temperature of $50^\circ C$ and added with sodium carbonate to a pH of 9 to get a precipitate of manganese carbonate.

2. Manganese Carbonate Calcination

The manganese carbonate obtained from the leaching process is then calcined in a tube furnace at $600^\circ C$ for 2 hours to obtain MnO_2 composite.

3. Manufacture of MnO₂/Carbon Powder

MnO₂/Carbon powder was prepared by weighing activated carbon and MnO₂ in various ratios (0 : 1), (0.25 : 0.75), (0.50 : 0.50), (0.75 : 0.25). The composition of PVDF : Acetylene black was added with a ratio of 0.1 : 0.1 as a binder polymer for each powder ratio.

4. Testing Using FTIR

Fourier Transform Infrared (FTIR) testing was carried out to determine the functional groups formed during the synthesis process. This test was carried out with a wavelength of 400 - 4000 cm⁻¹.

5. Materials Characterization

The MnO₂/Carbon sample was tested by X-Ray Diffraction (XRD) to identify the crystal structure of the powder material. This measurement uses a Cu-K target anode ($\lambda=1.54056 \text{ \AA}$) and is carried out at an angle of 2θ (10°–90°). The characterization of the phase content begins with a qualitative analysis of the resulting pattern on XRD, which works by utilizing Bragg's Law.

6. LCR-Meter Testing

Weighed the MnO₂ Composite: Activated Carbon with each ratio (1 gr : 0 gr), (0.27 gr : 0.25 gr),

(0.5 gr : 0.5 gr) and (0.25 gr : 0.75 gr), (0 gr : 1 gr), then add water one and PVA glue to form a slurry. Then the slurry that has been stirred evenly is smeared with two sheets of aluminum foil electrodes with a plate size of 3 x 3 cm². Furthermore, the electrode sheet that has been smeared is heated in a kirin oven with a temperature of 105°C until dry. Furthermore, the two electrode sheets are faced and given a paper membrane that has been dissolved in sodium sulfate electrolyte solution. The series of electrode sheets that have been completed are then tested using an LCR-Meter to determine the values of capacitance (C), inductance (L), and resistance (R) (Alwin, 2020).

7. Conductivity Testing on Manganese-Activated Carbon

Weighed MnO₂: Activated carbon (0.50 gr : 0.50 gr) was added to 50 mL of ethanol and stirred for 2 hours. In the same way, the ratio of MnO₂-Graphene (1 gr : 0 gr), (0.75 gr : 0.25 gr), (0.25 gr : 0.75 gr), (0 gr : 1 gr), put 50 mL of ethanol and stirred for 2 hours. Results of Manganese-Activated Carbon solutions in various comparisons (1 gr : 0 gr), (0.75 gr : 0.25 gr), (0.50 gr : 0.50 gr), (0.25 gr : 0.75 gr), (0 gr : 1 gr), tested for conductivity using a Conductometer.

3. RESULTS AND DISCUSSION

3.1 Research Result

1. FTIR test

a. Manganese Oxide (MnO₂)

Table 1. FTIR Absorption

MnO ₂	Functional groups	Absorption Area (cm ⁻¹)
479,44	Mn-O	450-950
618.35	Mn-O	450-950
877,47	Mn-O	450-950
992.07	Mn-O	450-950
1104,27	CO	1080-1390
1190.69	CO	1080-1390
1384,21	CO	1080-1390
1438,44	OH Bends	1528-1700
1627,70	OH Bends	1528-1700
3398,29	Oh Stretching	3550-3200

a. XRD test

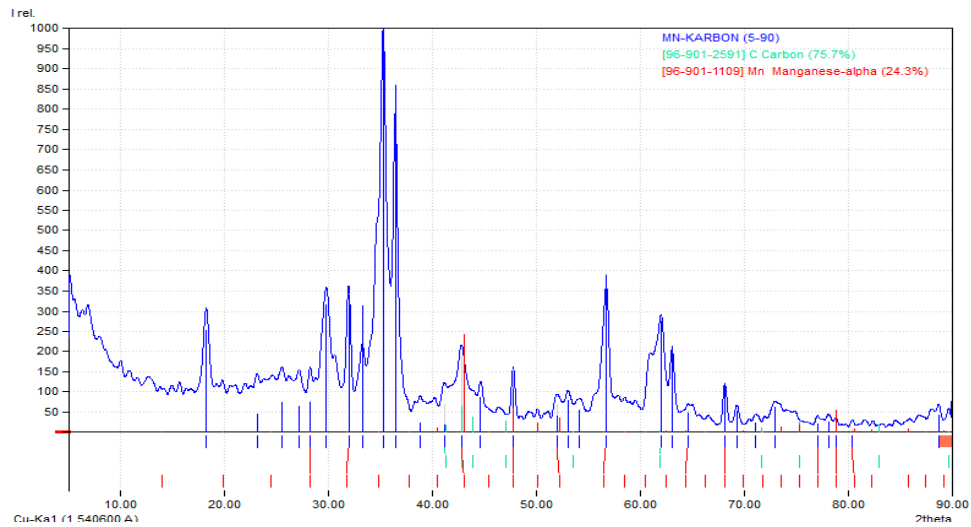


Fig. 1. Diffraction pattern XRD analysis of MnO₂-Carbon composites

2. Test LCR Meter

a. Capacitance Test (μF)

Table 2. MnO₂-Carbon Capacitance Test

Capacitance (μF)				
Variation MnO ₂ : Carbon	Simplo	Duplo	Triplo	Average
1 : 0	09,8	10,5	10,8	10,4
0.75 : 0.25	15,8	16,2	16,3	16,1
0.50 : 0.50	64,5	64,8	64,6	64,6
0.25 : 0.75	65,5	65,3	65,1	65,3

b. Inductance Test (mH)

Table 3. MnO₂-carbon inductance test

inductance (mH)				
Variation MnO ₂ : Carbon	Simplo	Duplo	Triplo	Average
1 : 0	19,7	19,4	18,9	19,3
0.75 : 0.25	126,3	124,6	129,4	126,7
0.50 : 0.50	0,14	0,12	0,12	0,12
0.25 : 0.75	09,6	09,2	09,4	09,4

c. Resistance Test (kΩ)

Table 4. MnO₂-carbon resistance test

Resistance (kΩ)				
Variation MnO ₂ : Carbon	Simplo	Duplo	Triplo	Average
1 : 0	3,44	3,69	3,69	3,60
0.75 : 0.25	11,08	11,19	11,01	11,09
0.50 : 0.50	9,45	9,42	9,59	9,48
0.25 : 0.75	1,89	1,94	1,93	1,92

3. Conductometer Test

Table 5. MnO₂-carbon conductivity test

Conductivity (µS CM-1)				
Variation MnO ₂ : Carbon	Simplo	Duplo	Triplo	Average
1 : 0	54,4	55,5	55,7	55,2
0.75 : 0.25	60,7	60,4	60,3	60,4
0.50 : 0.50	49,8	50,5	50,4	50,2
0.25 : 0.75	28,9	27,2	27,2	27,7

4. DISCUSSION

4.1 Manganese Rock

Manganese stone was taken in the Paludda area, Barru Regency, South Sulawesi. This manganese stone is washed using distilled water which aims to remove impurities attached to the manganese stone. The manganese stone is then dried in an oven at a temperature of 60-90°C so that the water content in the stone is reduced before grinding. The dried samples were then crushed to make the samples into powder. After obtaining the sample in powder form, it is sieved using a 150 mesh sieve to separate the coarse and fine sample particles.

4.2 Leaching of Manganese Ore

Leaching manganese rock through a hydrometallurgical process with sulfuric acid (H₂SO₄) as a solvent or leaching reagent and molasses as a reducing agent. Judging from previous studies that have been carried out by (Zhang et al. 2013), it is known that sulfuric acid (H₂SO₄) is effectively used in the manganese leaching process because it requires a reducing agent that will reduce this manganese rock from Mn⁴⁺ to Mn²⁺ so that it can dissolve in acids during the process leach. The hydrometallurgical process has advantages such as the relatively low cost, the small amount of reagent used, and is environmentally friendly. This study follows the optimization conditions of manganese washing from several previous studies, one of which is a study conducted by Korbafo (2017) where the difference from this study is in the reductor, namely Korbafo using teak sawdust in his research while in this study using molasses.

A total of 25 g of the prepared sample was added to 500 mL of 2 M H₂SO₄, stirred at 90°C, and added 50% molasses as a reducing agent. The leaching time was carried out for 6 hours because it was very effective and stirred using a

magnetic stirrer at 300 rpm. Then the mixture was filtered, and the leaching solution was heated at 70°C and added with 10% NaOH until the pH reached 5 – 6 to precipitate metal impurities. Then the solution was filtered, heated to a temperature of 50°C, and added with sodium carbonate to a pH of 9 to obtain manganese carbonate precipitate to produce filtrate and residue. The filtrate obtained is discarded, and only the residue is taken in the second and third screening processes. The residue obtained in the leaching process was analyzed using FTIR.

4.3 Manganese Carbonate Calcination

Manganese carbonate (MnCO₃) is produced from a leaching process that uses a 10% NaOH solution at a temperature of 70°C until the pH reaches 5-6. Sodium carbonate is added to precipitate the metal impurities at a temperature of 50°C in order to obtain manganese carbonate. Then it was calcified at 600°C for 2 hours to obtain a manganese oxide (MnO₂) composite.

4.4 Fourier Transform Infra-red (FTIR)

Functional group analysis with Fourier Transform Infra-Red (FTIR) from the electrodes is needed to determine the molecular bonds in the powder. The FTIR results obtained the resulting spectrum as shown in table 4.1, where the table shows the sample's transmittance spectrum and four functional group peaks. Three peaks with moderate transmittance are visible at wavelengths of 3192.2 cm⁻¹, 1614.61 cm⁻¹, and 1012.19 cm⁻¹. Meanwhile, there is a low transmittance peak at a wavelength of 479.44 cm⁻¹. The determination of the manganese oxide functional group and its purity is shown in Fig. 2. The infrared spectrum of the K-type manganese oxide *birnessite* shows peak Typical wave numbers are 479.44 cm⁻¹, 618.35 cm⁻¹, 877.47 cm⁻¹, and 992.07 cm⁻¹. This matter indicates the stretching of the Mn-O bonds in the octahedral layers of the structure *birnessite*. Previous studies also support this result, which explains

that wave numbers 413 cm^{-1} to 993 cm^{-1} are specific for the Mn-O bond. Tape absorption also appears at wave numbers 1104.27 cm^{-1} , 1190.69 cm^{-1} , and 1384.21 cm^{-1} , which indicates the CO group. This data is also supported by previous studies which show the existence of stretching CO (hydroxyl, ether, ester, or carboxylic acid) at wave numbers $1100\text{--}1400\text{ cm}^{-1}$. The absorption bands are at wave numbers 1438.44 cm^{-1} and 1627.70 cm^{-1} showing vibration *bending* from the OH group. The absorption band at wave number 3398.29 cm^{-1} is vibration stretching. This OH vibration describes the absorption band at wave number 3398.29 cm^{-1} and shows the presence of OH groups from the K-Br pellets bonded to metals in the interlayer.

1. X-Ray Diffraction (XRD)

MnO_2 is defined as a particle that tends to have an amorphous or low crystalline structure. In this study, $\alpha\text{-MnO}_2$ was chosen as the crystallinity structure as the best crystallinity parameter. conditions used.

Affect the crystallinity obtained from MnO_2 nanoparticles. Due to the formation of $\alpha\text{-MnO}_2$, $\beta\text{-MnO}_2$, $\gamma\text{-MnO}_2$ and $\delta\text{-MnO}_2$ can be stable under certain conditions. In this test, using XRD with an angle of 2θ from range $5^\circ\text{--}90^\circ$.

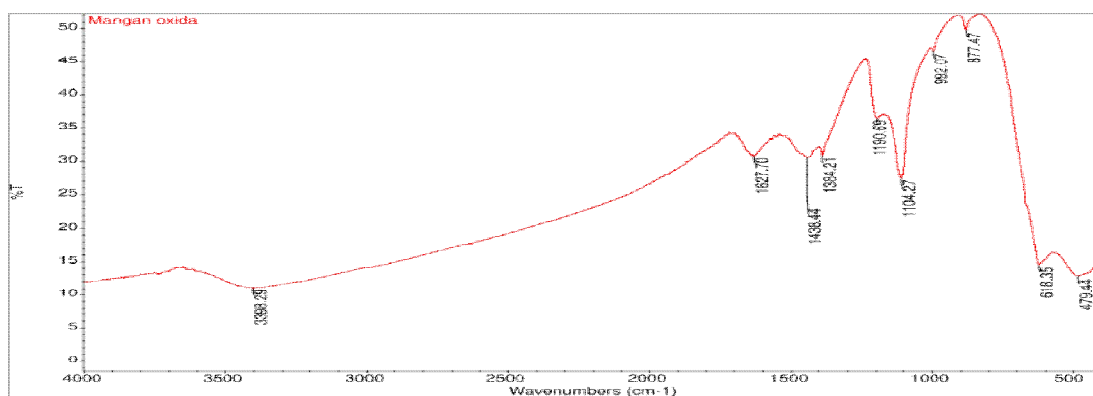


Fig. 2. FTIR graph of MnO_2 from manganese rock leaching

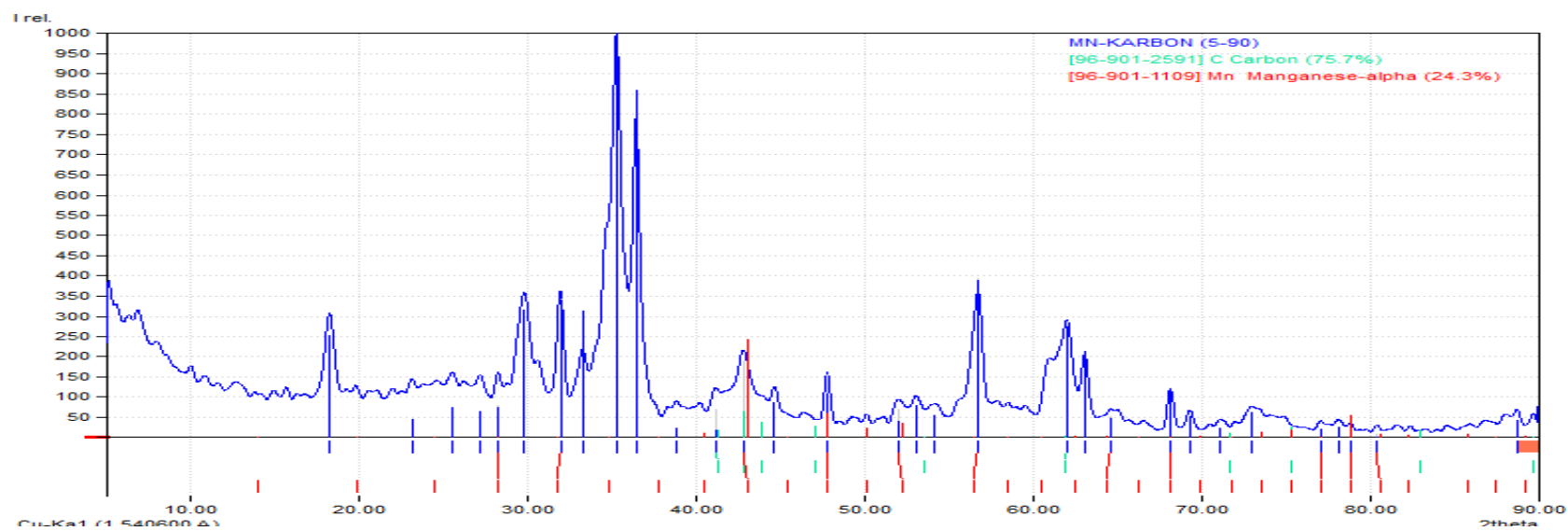


Fig. 3. MnO₂-Carbon Composite XRD Results

Based on Fig. 3, alpha manganese and carbon percentages are around 24.3% and 75.7%, respectively. It indicates that the difference in composition between manganese and carbon is quite high. These data indicate a significant shift in composition between MnO₂ and carbon. This difference is due to the temperature/temperature factor and the air component (CO₂). It resulted in MnO₂ undergoing oxidation due to CO₂ (environmental) factors, in which the element carbon (C) predominates. At the same time, graphene will experience an increase in composition due to the addition of carbon elements. Based on the results of the XRD data, the purity of the composition of MnO₂ and graphene is about 24.3% manganese (Mn) and 75.7% carbon. It shows that the percentage of composite MnO₂ and carbon can change if it is influenced by air (environment).

XRD data was generated at absorption peaks from the composite of MnO₂ and carbon. The highest peak was obtained at 35.28° with a peak of 1000.00. the peak reads the crystal lattice of carbon. Meanwhile, the second highest peak is at angle 2θ 36,46° with a peak of 859.71. At the peak, the crystal lattice of MnO₂ is read. Corner 2θ produced by each composite between carbon and MnO₂ has different characteristics. The crystal structure produced by carbon is hexagonal with six corner lattice sides. Meanwhile, the crystal lattice produced by MnO₂ is a face-centered cubic (cubic). The two crystals of the MnO₂-carbon composite have the characteristic of being amorphous. More

specifically, the MnO₂ crystal has a stable angular tendency because the distance between the lattice within the crystal is relatively the same, so it tends to have the best crystallinity (Rakhmad and Rakhma, 2018).

2. LCR-Meter test

a. Capacitance Test

On testing, this conducted testing with measure capacitance (C) for know capacity payload electricity stored. Measurement was conducted on plate-sized 2 x 2 cm² with thick series of 1 mm.

The results of the capacitance value in Graph 4 show the highest value produced is 65.3 μF in the composite ratio MnO₂: Carbon 0.25 g : 0.75 g, while the composite ratio MnO₂: Carbon 0.5 g : 0.5 g produces a capacitance value of 64.6 μF. Comparing the MnO₂: Carbon composite 0.75 g : 0.25 g produces a massive difference with a capacitance value of 16.1 μF, and MnO₂ 1 g has the lowest capacitance value of 10.4 μF.

b. Resistance Test

Resistance or obstacle electricity compared backward with conductivity or shipping. If the resistance is the value of what is the resistance of the electric current, so conductivity is the score of how much big he delivers current electricity. With principle, it could be formulated that magnitude conductivity is proportional turned against resistance (Sarwito, 2017: 16).

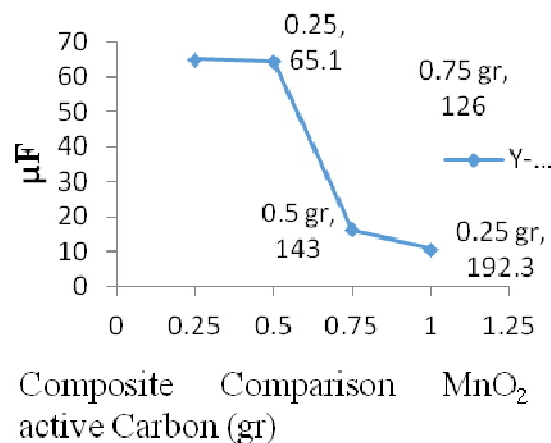


Fig. 4. Capacitance Value (C)

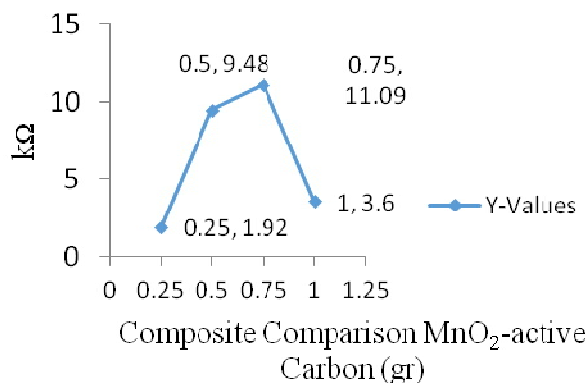


Fig. 5. Resistance Value (R)

The results of the resistance test values in Figure 5 shows the lowest resistance value in the comparison of the MnO₂ : Carbon 0.25 g : 0.75 g composite with a resistance value of 1.92 kΩ. Composite comparison MnO₂ : Carbon 0.5 g : 0.5 g resulted in a resistance of 9.48 kΩ. Composite comparison MnO₂ : Carbon 0.75 g : 0.25 g produces a high resistance of 10.9 kΩ. The ratio of MnO₂ 1 g produces a resistance value of 3.60 kΩ.

c. Inductance Test

Inductance becomes characteristic of suite electronic, which causing formation potential electricity compared with the current which flows through it is known as inductance self. Whereas if a change in the second current causes the electric potential of the circuit is called mutual inductance (Sarwito, 2017: 18).

The test results for the inductance value on the graph with the highest value are 126.7mHon the composite ratio MnO₂: Carbon 0.75 g : 0.25 g. Test value 19.3mHon the composite ratio MnO₂ : Carbon 1 g : 0 g. at a ratio of 0.25 g : 0.75 g has an inductance value of 09.4mH. In the comparison of the composite MnO₂: Carbon 0.50 g : 0.50 g obtained the lowest inductance with a value of 0.12 mH.

3. Conductivity Test

Conductivity analysis on 1 g MnO₂ sample variations, MnO₂: Carbon composite with various ratios of 0.75 g : 0.25 g, 0.5 g : 0.5 g, and 0.25 g : 0.75g. This test used a conductometer with the addition of 50 mL pa of ethanol solution to a variety of samples.

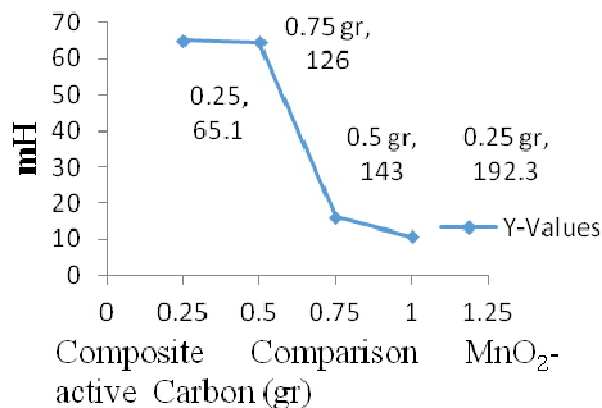


Fig. 6. Inductance Value (L)

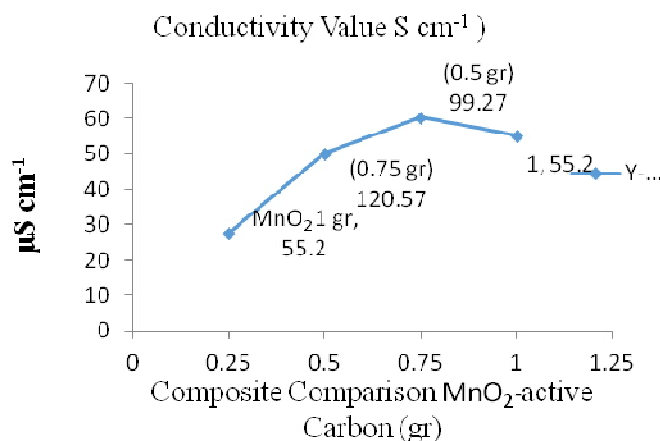


Fig. 7. Conductivity Value

The results of the conductivity value test on the graph obtained the highest conductivity value of 60.4 $\mu\text{S cm}^{-1}$ in the composite ratio MnO₂: carbon 0.75 g : 0.25g. In comparing the MnO₂ : carbon 0.5 g : 0.5 g composite, the difference in conductivity values was not much different from the conductivity value of 50.2 $\mu\text{S cm}^{-1}$. At a ratio of 1 g, MnO₂ has a conductivity value of 55.2 $\mu\text{S cm}^{-1}$. In the comparison of the MnO₂ : carbon composite 0.25 g : 0.75 g had the lowest conductivity value with a conductivity value of 27.7 $\mu\text{S cm}^{-1}$.

5. CONCLUSION

1. Synthesis of carbon MnO₂ was obtained from the leaching process using sulfuric acid (H₂SO₄), 50% molasses, 10% sodium hydroxide (NaOH), and sodium carbonate (Na₂CO₃), which produced a precipitate of manganese carbonate (MnCO₃).
2. Manganese (MnO₂) carbon in the FTIR test showed the presence of octahedral bonds in the birnessite structure, while in the XRD test, a hexagonal-shaped carbon crystal structure with six corner lattice faces and cubic face-centered MnO₂ crystals was obtained. These crystals have amorphous properties, affecting the resulting capacitance, inductance, resistance, and conductivity values. The highest capacitance value produced was 65.3 μF in the composite ratio MnO₂ : Carbon 0.25 g : 0.75. In the resistance test, the lowest resistance value was obtained in the comparison of the composite MnO₂ : Carbon 0.25 g : 0.75 g with a resistance value of 1.92 k Ω . The highest inductance value obtained was

126.7mHon the composite ratio MnO₂: Carbon 0.75 g : 0.25 g. In the conductivity test, the highest value was obtained at 60.4 $\mu\text{S cm}^{-1}$ in the composite ratio MnO₂: carbon 0.75 g : 0.25 g.

COMPETING INTERESTS

Authors have declared that no competing interests exist.

REFERENCES

1. Alamsah I, Puryanti D. Purification of manganese oxide with selective precipitation methods using Carbon. J FisUnand. 2019;8(4):348-54.
2. Agustin. Synthesis and characterization of MnO₂ doped with Fe³⁺ as an energy storage electrode [thesis]. Malang: State Islamic University of Maulana Malik Ibrahim Malang; 2019.
3. Aknanta FAJ. Analysis of inductance, resistance and capacitance measurements with maxwell inductance, maxwell capacitance Bridge and Anderson Bridge accompanied by the making of bridge circuits in the electrical laboratory and shipping system automation. Essay. Surabaya: Institute of Technology, 2017.
4. Ariyanto T, Prasetyo I, Rochmadi. The effect of pore structure on electrode capacitance of supercapacitors made from nanoporous Carbon. J Reactor. 2012;14 (1):25-32.
5. Desmulyati, Irawan A. Surface mount device capacitor calculation applications. J Prosisco. 2018;5(1):9.

6. Jablonskiene J, Simkunaite D, Vaiciuniene J, Stalnionis G, Drabavicius A, Jasulaitiene V et al. Synthesis of carbon-supported MnO₂ nanocomposites for supercapacitors application. *Crystals*;11(7):2021. DOI: 10.3390/cryst11070784
7. Matos CT, Ciacci L, Leon G, MF, Lundhaug M, Dewulf J et al. Material System Analysis of Five Batteryrelated Raw Materials: Cobalt, Lithium, Manganese, Natural Graphite, Nickel. DOI: 10.2760/519827, 2020
8. Muhlis WS, Bakri H. Estimation of manganese deposits using geoelectrical methods (soil types) in the Bonehau area PT. Manakarramulti mining, Mamuju regency, West Sulawesi Province. *J Geomine*. 2015;01(4):14-6.
9. Mustofa PD, Budiman A. Analysis of the influence of the sintering process on the structure of manganese ore derived from Nagari aie Ramo, kamang Baru District, Sijunjung regency. *J Phys Unand*. 2018;7(3):195-201.
10. Nursiti N, Wibowo ER, Safitri S, Oktavina R. Electrosynthesis of α -MnO₂/C nanocomposites and their fabrication for supercapacitor applications. *J Chemurg*. 2018;2(1):6. DOI: 10.30872/cm.g.v2i1.1631
11. Dinda Al Qory R, Zainuddin Ginting BS. Refining used oil using activated carbon from Salak seeds (*Salacca zalacca*). *J Teknol Kim Unimal*. 2012;2(1):26-36.
12. Saridewi N, Arif S, Alif A. Synthesis of manganese oxide nanomaterials using solvent-free methods. *J Kim*. 2015;1 (Nov):117-23. DOI: 10.15408/jkv.v0i0.3147.
13. Sasongko W, Idrus A, Ariza IS. 'Geology and mineralization characteristics of manganese ore in the Cileutak area, Simpenan District, Sukabumi Regency, West Java Province' *J The. 5th Annual Engineering seminar*. 2014;5(1):177-83.
14. Solihin S, Wibawa A. The transformation of pyrolusite minerals at high temperatures. *J Technol Miner Coal*. 2018;14(3):179-86. DOI: 10.30556/jtmb.vol14.no3.682
15. Sujatno A, Salam R, Bandriyana DA. Scanning electron microscopy (Sem) study for the characterization of zirconium alloy oxidation processes. *J Nukl Forum*. 2015;9(1):44. DOI: 10.17146/jfn
16. Leto TK. Leaching of manganese ore from East Nusa Tenggara using hydrolyzed sawdust as A reductant with sulfuric acid solvent. *Essay*. Surabaya: Institute of Technology, 2017.
17. Chanif M, Sarwito IS, K ES. "Analysis of Adding Capacitors to the Charging Process of Undersea Vehicle Batteries". *J POMITS. Engineering* 289795519. 2014; 3(1):1-6.
18. Siagian W. Analysis of the working principles of charge and discharge processes on capacitors with Rc circuits. *J Ilm Simantek*. 2020;4(2):44-53.
19. Wahyuni Andi NU. Synthesis of manganese dioxide nanoparticles (MnO₂) sonochemically as an adsorbent for lead metal ion (Pb²⁺) [thesis]. Makassar: UINAM; 2017.
20. Wang J-W, Chen Y, Chen B-Z. A synthesis method of MnO₂/activated carbon composite for electrochemical supercapacitors. *J Electrochem Soc*. 2015;162(8):A1654-61. DOI: 10.1149/2.0031509jes
21. Wira Wayan IY, Ibrahim Malik FM, Masruroh UNM, Valiana V, Triandi R. Supercapacitor electrodes made from MnO₂/AC nanocomposites from plastic waste using electrodeposition technique. *J Process Integr*. 2021;10(2): 77-81.
22. Zainuri A, Mulyasuryani A. Development of a conductivity-based instrument for detecting fir food in agricultural products. *J Auto.Ctrl.Inst*. 2016;8(2): 240.
23. Tetra O.N, Aziz H. Emriadi, Ibrahim S, Alif A. Supercapacitors Made Activated Carbon Ionic Solut Electrolytes *J Zarah*. 2018;6(1):39-46. DOI: 10.31629/zarah.v6i1.293
24. Sumardi S, Mubarak MZ, Saleh N. Processing of manganese ore into manganese sulfate through reductive leaching using oxalic acid in an acidic environment. *J Proc Semirata FMIPA Univ Lampung*. 2013;2(1):123-30.
25. Sumardi S, Mufakhir FR, Prasetyo AB. Study of leaching kinetics of low content manganese ore in Way Kanan, Lampung using molasses in acidic conditions. *J Metall*. 2014;29(2):111. DOI: 10.14203/metalurgi.v29i2.282
26. Tetra O.N, Aziz H. Emriadi, Ibrahim S, Alif A. Supercapacitors Made Activated Carbon Ionic Solut Electrolytes *J Zarah*. 2018;6(1):39-46. DOI: 10.31629/zarah.v6i1.293

27. Triyono, Sajima. Leaving of Leburan Sand Zircon Kalimantan using bench scale hot water. J Forum Nuklis. 2017;11(1): 1-6.
28. UI-Hamid Anwar. A beginners' guide to scanning electron microscopy. Dhahran, Saudi Arabia: Center For Engineering Research, King Fahd University Of Petroleum & Minerals. 2018.
29. Subagio A, Priyono P, Yudianti R. Characterization of CNT/MnO₂ nanocomposite materials for supercapacitor material applications. J Phys Indones Educ. 2014;10(1): 92-103.
DOI: 10.15294/jpfi.v10i1.3056
30. Maddu A, Saputra A, Ayuningtiyas NI, Tsalsabila A, Ismayana A, Nurhalim ArjoS. Synthesis of MnO₂/Carbon dots nanocomposite derived from rice Husk for supercapacitor electrodes. Int J Renew Energy Res. 2018;8(3):1476-82.

© 2022 Author name; This is an Open Access article distributed under the terms of the Creative Commons Attribution License (<http://creativecommons.org/licenses/by/4.0>), which permits unrestricted use, distribution, and reproduction in any medium, provided the original work is properly cited.